High-mobility semiconducting polymers with different spin ground states

Xiao-Xiang Chen
Peking University
Jia-Tong Li
Peking University
Yu-Hui Fang
Peking University
Xue-Qing Wang
Peking University
Guangchao Liu
Peking University
Yunfei Wang
University of Southern Mississippi https://orcid.org/0000-0001-7555-5308
Xin-Yu Deng
Peking University
Xiaodan Gu
The University of Southern Mississippi https://orcid.org/0000-0002-1123-3673
Shang-Da Jiang
South China University of Technology https://orcid.org/0000-0003-0204-9601
Ting Lei (tinglei@pku.edu.cn)
Peking University https://orcid.org/0000-0001-8190-9483

Article

Keywords: semiconductors, polymers, spin ground states

Posted Date: August 13th, 2021

DOI: https://doi.org/10.21203/rs.3.rs-764062/v1

Abstract

Organic semiconductors with high-spin ground states are fascinating because they could enable fundamental understanding on spin-related phenomenon in light element and provide opportunities for organic magnetic and quantum materials. Although high-spin ground states have been observed in some quinoidal type small molecules or doped organic semiconductors, semiconducting polymers with high-spin at its neutral ground state are rarely reported because of the less of clear design strategy. Here we propose a molecular design strategy to obtain high-mobility semiconducting polymers with different spin ground states. We show that polymer building blocks with small singlet-triplet energy gap (ΔE_{S-T}) could enable small ΔE_{S-T} gap and increase the diradical character in copolymers. We first demonstrate that the spin density and solid-state interchain interactions in the high-spin polymers are crucial for their ground states. Polymers with a triplet ground state (S = 1) could exhibit doublet (S = 1/2) behavior due to the solid-state interchain spin-spin interactions. Besides, these polymers showed outstanding charge transport properties with high hole/electron mobilities and can be both n- and p-doped with superior conductivities. Our results demonstrate a rational design approach to high-mobility semiconducting polymers with different spin ground states.

Introduction

π-Conjugated organic molecules with open-shell or high-spin ground state have attracted increasing interests due to their unique optoelectronic and magnetic properties[1,2,3]. However, these molecules contain unpaired electrons and are often unstable compared with the closed-shell molecules because they can easily form dimers, or being quenched due to their high reactivity. Recently, many efforts have been devoted into the development of stable open-shell conjugated molecules. And related strategies include the use of large steric hindrance groups to protect unpaired electrons, and delocalization of unpaired electrons to large conjugated systems[4]. Based on these strategies, some open-shell π-conjugated organic molecules, including *p*-quinodimethanes (QDMs)[5], polycyclic aromatic hydrocarbons (PAHs), quinoidal oligothiophene derivatives (QOTs)[6] were investigated (Fig. 1a). Recent works on the design and precise synthesis of open-shell small molecules and oligomers have greatly expanded the open-shell small π-conjugated organic molecule library and provide more in-depth understanding on their optoelectronic and magnetic properties[7,8,9,10,11].

Charge carrier mobility is a critical parameter for an optoelectronic device, which reflects the speed at which the charge carriers move in a material. Open-shell organic molecule with high mobility will enable long spin transport distance which is crucial for spin-related applications[12,13,14]. However, there are few reports of small open-shell molecules with high charge carrier mobilities[10,15,16,17]. This is because the use of steric hindrance groups prevents close packing of molecules, and increasing the conjugation length requires more complex synthetic steps. Figure 1b shows some representative π-conjugated open-shell molecules, which usually show charge carrier mobilities only around 10^{-3} cm^2 V^{-1}. The low charge

carrier mobilities of these molecules greatly restrict their applications in optoelectronic and spin-related devices.

Conjugated polymers have been intensively studied for various optoelectronic applications because of their high mechanical flexibility/stretchability and large-scale solution processability.[18,19,20] In the past decade, development of high-performance polymer building blocks, including indacenodithiophene (IDT)[19], naphthalene diimide (NDI)[21], diketopyrrolopyrrole (DPP)[22], isoindigo (IID)[23], and benzodifurandione-based oligo(p-phenylene vinylene) (BDOPV)[24], have greatly promote the charge carrier mobility enhancement in conjugated polymers. Conjugated polymers with open-shell character can be obtained by chemical doping[25]. However, the doped polymers are unstable and the ionized dopants always result in large structural and energetic disorders.[26] In addition, doped semiconducting polymers are always conductors while losing their semiconducting properties. Recently, conjugated polymers at its neutral ground state were reported to have open-shell high-spin character[27,28], but these polymers showed conducting properties with limited applications in semiconducting devices. To date, the guidelines for the design of these polymers are rarely explored, and the influential factors for their spin properties are still obscure.

Here we report a strategy to design high-spin ground state and high-mobility semiconducting polymers. This approach is based on three assumptions: (i) most high-mobility conjugated polymers are based on several high-performance building blocks (e.g. NDI, IID, and DPP *etc. Figure2*a), and thus these building blocks are needed; (ii) as the singlet-triplet energy gap (ΔE_{S-T}) value increase, the stability of the high-spin triplet state will increase, and the triplet state may become the ground states in some molecules[5]; (iii) the polymers need to have a highly planar backbone, which can lead to better conjugation, smaller ΔE_{S-T}, and also benefits charge transport. Based on these assumptions, we screened currently available high-performance polymer building blocks by calculating their ΔE_{S-T} values and planarity indexes. Three polymers were synthesized for comparison. These polymers exhibit distinct magnetic properties and solid-state spin-spin interactions. Among them, p(TDPP-TQ) and p(TDPP-BBT) exhibit air-stable triplet ground state. Moreover, p(TDPP-TQ) displays high electron mobilities of up to 7.76 $cm^2 V^{-1} s^{-1}$ and high hole mobilities of up to 6.16 $cm^2 V^{-1} s^{-1}$. Interestingly, the polymer can also be effectively n-doped and p-doped, showing outstanding n-type and p-type electrical conductivities (σ_e=16.1 S/cm and σ_h=348.3 S/cm).We believe that our design strategy could help to discover more high-mobility semiconducting polymers with different spin ground states.

Results And Discussion

To date, many high-mobility semiconducting polymers are based on the copolymerization of “large fused aromatics” and “small-size aromatics”. Thus, we collected potential polymer building blocks from recently published reviews[22,29] and separate them into two groups: “large fused aromatics” and “small-size aromatics” (Fig. 2a-b). Based on the above assumptions, we first performed DFT calculations to obtain their ΔE_{S-T} values. Among all the building blocks, TDPP, BDOPV, TQ and BBT exhibits the smallest ΔE_{S-T}.

Then, we performed DFT calculations to estimate the planarity of the polymer building block combinations by using a recently developed planarity indexes $\langle\cos^2\varphi\rangle$[30]. We found that TDPP can form planar polymer backbone with TQ and BBT with high torsional barriers and large $\langle\cos^2\varphi\rangle$ (Fig. 1c). Whereas when BDOPV was copolymerized with TQ and BBT, the resulting polymers show small $\langle\cos^2\varphi\rangle$ values, suggesting the polymers significantly deviate from planarity (Fig. S2). Backbone planarity is important for good conjugation and also crucial for efficient intra- and interchain charge transport. To have a systematically understanding of the relationship between molecular structure and open-shell property, we choose TDPP as the "large fused aromatic", and BT, TQ and BBT with decreased $\Delta E_{S\text{-}T}$ values, as the "small-size aromatic" to construct polymers. Note that TDPP, BT, TQ and BBT are usually consider as "acceptors" in conjugated polymers. Unlike traditional donor-acceptor design[27], this "acceptor-acceptor" design allows the polymers to have enough bandgap to show semiconducting rather than conducting property.

The three polymers, p(TDPP-BT), p(TDPP-TQ) and p(TDPP-BBT), were synthesized via Pd-catalyzed Stille polymerization reaction between the trimethyltin TDPP and the dibromo compounds of BT, TQ and BBT (Fig 3a). The synthesis and purification procedures are detailed in Supplementary Materials. The stability of those polymers was proved by thermogravimetric analysis, and all the polymers showed high decomposition temperatures over 350 ℃ (Fig. S4). Three polymers show gradually red-shifted absorption spectra as decreasing the $\Delta E_{S\text{-}T}$ of the "small-size aromatic" (Fig. 3b). The HOMO/LUMO energy levels of p(TDPP-BT), p(TDPP-TQ) and p(TDPP-BBT) obtained by cyclic voltammogram (CV) measurements are −5.34/−3.55, −5.23/−3.94, and −5.20/−4.17 eV, respectively (Fig. S3 in SI). The increase of the HOMO and the decrease of the LUMO level is probably due to the enhanced planarity, better conjugation, and more readily aromatic-to-quinoidal transformation (Fig. 3c and Fig. S2).

The high-spin characteristics of the polymers were investigated by electron paramagnetic resonance (EPR) and superconducting quantum interference device (SQUID) both in solution and in solid state. At room temperature, the solid-state EPR intensity increases dramatically in the order of p(TDPP-BT), p(TDPP-TQ) and p(TDPP-BBT) (Fig. 4a), which reflects an increasing of spin density. More importantly, the EPR intensities showed negligible change after storing the polymers in air for 90 days, suggesting the high air stability of these open-shell polymers (Fig. S5). The EPR intensity of p(TDPP-BT) is very weak and shows a closed shell feature, and thus we will not study this polymer in detail. To compare the spin dynamics of p(TDPP-TQ) and p(TDPP-BBT), temperature-dependent EPR measurements in solid state were performed (Fig. 4b, S5a). Their EPR intensities decrease with the increase of temperature, suggesting that they probably have a triplet ground state[1]. It is known that if there exists a triplet state ground state, the EPR signal of $|\Delta m_s| = 2$ forbidden transition can be observed, even with very weak intensity[1]. To determine the existence of triplet ground state in the polymers, the $|\Delta m_s| = 2$ forbidden transition is measured. For p(TDPP-BBT), a low intensity but clear signal at $|\Delta m_s| = 2$ is observed (Fig. 4c), suggesting the existence of triplet ground state. For p(TDPP-TQ), the forbidden transition could not be observed, which is largely due to its relatively weak EPR intensity compared to p(TDPP-BBT). Furthermore, the variable temperature EPR of both polymers in solution were also measured and showed

a similar behavior compared to solid state EPR. The EPR intensities of p(TDPP-TQ) and p(TDPP-BBT) decrease with the increase of temperature (Fig. 4d, S5b). The EPR data of p(TDPP-BBT) from 4.9 K to 50 K were fitted by Bleaney-Bowers equation, which provides an energy gap between singlet and triplet ($\Delta E_{S\text{-}T}$) of 4.92×10^{-3} kcal mol^{-1} (J = 0.86 K) (Fig. 4e).

To further investigate the static magnetic properties of the polymers, temperature–dependent magnetic susceptibility was measured by SQUID from 2 K to 300 K under DC field (Fig. 4f). The values of the product of magnetic susceptibility and temperature ($\chi_M T$) increase linearly with temperature. This feature usually suggests strong antiferromagnet coupling or temperature-independent paramagnetism (TIP). Due to the relatively low calculated spin density and weak spin-orbit coupling in organic polymers, this phenomenon is usually attributed to TIP[31,32]. TIP comes from Curie and Pauli paramagnetism ($\chi_{total} T$ = C + $\chi_{Pauli} T$), where C is Curie paramagnetism and T is temperature. For organic molecule, Curie paramagnetism is negligible. Thus, we can calculate the χ_{Pauli} of p(TDPP-TQ) and p(TDPP-BBT) to be 8.2×10^{-4} and 3.5×10^{-3} cm^3/mol, respectively. From the relation $\chi_{Pauli} = \mu_B{}^2 N(E_F)$, where μ_B is the Bohr magneton, the densities of states at the Fermi energy $N(E_F)$ for those p(TDPP-TQ) and p(TDPP-BBT) were calculated to be 1.5×10^{22} and 6.5×10^{22} eV^{-1} cm^{-3}. The Pauli paramagnetism and large value of $N(E_F)$ reveal that the spins in these polymers are highly delocalized.[33,34] In particular, for p(TDPP-BBT), the $\chi_M T$ and T are slightly deviated from the linear relationship at low temperature (red circle in Fig. 4f). This behavior could be due to the weak antiferromagnetic coupling between polymer chains, which we will prove later by studying the aggregation behavior of the polymers. To determinate the spin ground state of those polymers, field-dependent magnetization measurements (M-H) were performed. For p(TDPP- TQ), it shows a close to S = 1 triplet state (Fig. 5a, S7), consistent with EPR results; while for p(TDPP-BBT), it shows a close to S = 1/2 doublet state in the measurement (Fig. 5b, S8). It seems that this result conflict with the EPR measurement. However, we will show that this phenomenon can be well explained with the high spin density and strong interchain interactions in p(TDPP-BBT).

It has been reported that conjugated polymers with rigid backbones are strongly aggregated even in dilute solutions[35,36]. The strong intermolecular interaction will affect spin delocalization[31]. To understand the polymer chain interactions, we performed the temperature-dependent UV-vis absorption spectra of p(TDPP-TQ) and p(TDPP-BBT) (Fig. S9-S10). We and others have shown that in good solvent (dissolving polymers better), conjugated polymers can be more readily disaggregated at elevated temperature[35,37]. Therefore, three solvents, toluene, *o*-dichlorobenzene (*o*-DCB), and 1-chloronaphthalene (1-CN), with increased solubility for conjugated polymers were used. For both polymers, the maximum absorption peak decreases with increasing temperature and decrease more significantly in good solvent, such as 1-CN, suggesting that both polymers are strongly aggregated in solution. The strong aggregation of the polymer supports the observed large $N(E_F)$ values, which could explain the TIP phenomenon. Previous study has shown that strong spin-spin interactions in triplet small molecules could result in doublet state in magnetization measurements[15]. p(TDPP-TQ) has a low spin density and direct spin-spin interaction can hardly happen (Fig. 5c), thus exhibiting a triplet ground state in solid state. In p(TDPP-BBT), the high

spin density makes the spin at the chain end can directly interact with each other, leading to an apparently doublet ground state, consistent with the field-dependent magnetization measurement. Therefore, both spin density and interchain interaction contribute to the observed different spin ground states.

To further understand the magnetic properties, density functional theory (DFT) calculations were performed on their oligomers (n = 6). The calculated $\Delta E_{S\text{-}T}$ of the oligomers were −19.50 kcal/mol for p(TDPP-BT), −3.69 kcal/mol for p(TDPP-TQ), and −0.14 kcal/mol for p(TDPP-BBT), which is consistent with the above observed trend that p(TDPP-BBT) could have very small $\Delta E_{S\text{-}T}$ value and a triplet ground state. The significant decrease of $\Delta E_{S\text{-}T}$ indicates the increased stability of the open-shell triplet ground state, which agrees well with the observed EPR results and magnetic property. The large absolute $\Delta E_{S\text{-}T}$ value of p(TDPP-BT) lead to the inaccessible of the triplet state even at room temperature. While for p(TDPP-TQ) and p(TDPP-BBT), the small $\Delta E_{S\text{-}T}$ value of their oligomers could make the polymers have triplet ground state if the polymers have high degree of polymerization and strong interchain interactions. The singlet diradical character index (y_0), which is often used to estimate the diradical property, was also calculated[38,39]. The value of y_0 ranges from 0 to 1; 0 means closed-shell, while y_0 = 1 stands for pure diradical. The calculated y_0 values of $(TDPP\text{-}BT)_6$, $(TDPP\text{-}TQ)_6$, and $(TDPP\text{-}BBT)_6$ are 0.012, 0.350, and 0.996 (Table S2-S4). The difference of the spin triplet states for each polymer can be visualized by the spin density distribution in Fig. 4g. From $(TDPP\text{-}BT)_6$ to $(TDPP\text{-}BBT)_6$, the triplet spin density distribution changes from localized in the center, to uniformly distributed along the chain, and to mostly distributed at the end of the chain. This result agrees well with the increase of the y_0 value (Fig. S13-S15). The Bond length alternation analysis (Fig. S16-S18) also shows that the bond length difference between open-shell singlet and triplet of $(TDPP\text{-}BT)_6$ become obvious only in the middle of molecule. For $(TDPP\text{-}TQ)_6$, it emerges throughout the entire oligomer. For $(TDPP\text{-}BBT)_6$, the bond length difference is negligible, which is consistent to its small $\Delta E_{S\text{-}T}$ value.

Based on the magnetic properties and DFT calculations, the following conclusion can be obtained: (1) p(TDPP-BT) has a singlet ground state because of its large $\Delta E_{S\text{-}T}$ value; (2) p(TDPP-TQ) and p(TDPP-BBT) all showed triplet ground state because of their oligomers' intrinsically small $\Delta E_{S\text{-}T}$ values; (3) Because of the strong interchain interactions and separately distributed spin-density in p(TDPP-BBT), it shows doublet state in field-dependent magnetization measurement; whereas the low spin density and relatively uniformly distributed spin density in p(TDPP-TQ) make it exhibit triplet state.

The charge transport properties of the polymers were evaluated by field-effect transistors (FET) with a top-gate/bottom-contact (TGBC) configuration (Fig. 6e, Fig. S1&Fig. S19-S21). Unlike previously reported high-spin polymers with conducting properties[27], our polymers show typical semiconducting properties with good ambipolar charge transport properties. The polymers also showed good on/off ratios if the V_{DS} is small. p(TDPP-BT) exhibits good electron mobilities of up to 3.83 $cm^2\ V^{-1}\ s^{-1}$ and hole mobilities of up to 2.77 $cm^2\ V^{-1}\ s^{-1}$. p(TDPP-TQ) exhibits high electron mobilities of up to 7.76 $cm^2\ V^{-1}\ s^{-1}$ and high hole

mobilities of up to 6.16 $cm^2 V^{-1} s^{-1}$. These values are the highest reported to date in high-spin ground state polymers, and also among the highest in all reported organic semiconductors[22]. p(TDPP-BBT) shows relatively lower electron mobilities of 0.25 $cm^2 V^{-1} s^{-1}$ and hole mobilities of 0.37 $cm^2 V^{-1} s^{-1}$. To date, only a few reported open-shell small molecules have shown moderate charge carrier mobilities, usually on the order of 10^{-3} $cm^2 V^{-1} s^{-1}$ (Fig. 1 and Table S5)[10,15,16,17,40]. Therefore, our approach successfully addressed the challenge to design high-mobility and high-spin ground-state organic semiconductors.

Grazing incidence wide-angle X-ray scattering (GIWAXS) and atomic force microscopy (AFM) were employed to study the microstructures and morphology of the polymer films. (Fig. 6a-6c). All the polymers show typical edge-on dominated molecular packing in solid state. p(TDPP-BT) shows the narrower full width at half maximum (FWHM) (Fig S24 and Table S6) with a lamellar distance of 21.67 Å and a π-π stacking distance of 3.57 Å, suggesting its higher crystallinity. p(TDPP-TQ) shows wider FHWM with a lamellar distance of 20.94 Å and a π-π stacking distance of 3.70 Å. For p(TDPP-BBT), it shows a similar lamellar distance of 21.67 Å but larger π-π stacking distance of 3.88 Å. AFM height images show that the polymer films have very smooth surface with root-mean-square surface roughness < 1 nm (Figure S22). Clearly, the charge transport properties of the three polymers are not strongly correlated with their molecular packings. This phenomenon is common in conjugated polymers, because many studies have shown that crystallinity and π-π stacking distance of polymers are not the only parameters affecting their charge transport properties, and other parameters, such as interchain short contacts[41], packing conformation[42], and energetic disorders[43], also strongly influences charge carrier mobilities.

Previous studies suggest that spin-spin interactions in materials could lead to enhanced thermopower in some thermoelectric materials[44,45]. Since organic thermoelectric materials are usually achieved under doped states, we explored the charge transport properties after doping. We found that p(TDPP-TQ) can be both effectively n-doped and p-doped. For n-doping, a commonly used n-dopant, *N*-DMBI, was used. After optimizing the doping concentration and annealing temperature, the n-type electrical conductivity of p(TDPP-TQ) polymer achieved 16.1 S/cm (Fig. 6e), which is among the highest in n-doped organic semiconducting polymers[46,47]. P-doping was performed by immersing p(TDPP-TQ) films in a 10 mM $FeCl_3$ solution. The polymer can be easily p-doped as observed in the UV–vis–NIR absorption spectra (Fig. S23). By varying the immersion time, the polymer showed a p-type electrical conductivity of 348.3 S/cm (Fig. 6f), which is also among the highest in p-doped conjugated polymers. One polymer that can achieve both high n-type conductivity and p-type conductivity after doping is rare in literature[48,49]. Such unique doping behavior of p(TDPP-TQ) could be probably due to the ease of accepting and donating electrons of the triplet state. These results also suggest the great potential of using high-spin semiconducting polymers in the applications requiring heavily doping, e.g. organic thermoelectrics and organic bioelectronics[48,50,51].

Conclusion

In summary, we have developed a rational strategy to screen the potential polymer building blocks for designing high-spin ground state and high mobility semiconducting polymers. Based on the strategy, three polymers with different spin ground state were obtained. We found that the highly delocalized spin and the strong interchain aggregation could lead to different spin behaviors for these polymers. p(TDPP-BT) has a singlet ground state, while p(TDPP-TQ) and p(TDPP-BBT) have a triplet ground state. More importantly, all these polymers showed high charge carrier mobilities among all the reported high-spin organic semiconductors, and they could also be readily p- and n-doped to show high electrical conductivities, suggesting their broad applications for versatile organic magnetic and electronic devices. We believe that the molecular design strategy developed in this work could bring more air-stable, high-spin and high-mobility semiconducting polymers with different ground states, which could enable broad spin-related applications beyond the current scope of organic electronics.

Declarations

Acknowledgements

This work is supported by National Natural Science Foundation of China (22075001), the Key-Area Research and Development Program of Guangdong Province (2019B010934001), and the Beijing Natural Science Foundation (2192020). The computational part is supported by High-performance Computing Platform of Peking University. X.G. and Y.W. thank NSF (OIA-1757220) for providing support to perform the scattering portion of this work. The authors thank Prof. Zhe-ming Wang, Prof. Hao-ling Sun, Ye-xin Wang, Dr. Shen Zhou for their kind help in SQUID and EPR measurement.

Author contributions

X.X.C. and J.T.L. contributed equally to this work. X.X.C. and G.C.L. synthesized the polymers. X.X.C. and X.Y.D. performed property characterization and DFT calculation. J.T.L. and X.Q.W. performed device fabrication and characterization. Y.W. and X.G. performed the X-ray scattering measurement and data analysis. Y.H.F. and S.D.J. performed EPR measurement. X.X.C., J.T.L., and T.L. wrote the manuscript. All the authors revised and approved the manuscript.

Additional information

The authors declare no competing financial or non-financial interests.

References

1. Abe M. Diradicals. *Chem. Rev.* **113**, 7011–7088 (2013).
2. Ai X, Evans EW, Dong S, Gillett AJ, Guo H, Chen Y, *et al.* Efficient radical-based light-emitting diodes with doublet emission. *Nature* **563**, 536–540 (2018).
3. Rugg BK, Krzyaniak MD, Phelan BT, Ratner MA, Young RM, Wasielewski MR. Photodriven quantum teleportation of an electron spin state in a covalent donor-acceptor-radical system. *Nat. Chem.* **11**,

981–986 (2019).

4. Ji L, Shi J, Wei J, Yu T, Huang W. Air-stable organic radicals: new-generation materials for flexible electronics? *Adv. Mater.* **32**, 1908015–1908030 (2020).
5. Casado J. Para-quinodimethanes: a unified review of the quinoidal-versus-aromatic competition and its implications. *Top. Curr. Chem.* **375**, 73 (2017).
6. Zhang C, Medina Rivero S, Liu W, Casanova D, Zhu X, Casado J. Stable cross-conjugated tetrathiophene diradical. *Angew. Chem., Int. Ed.* **58**, 11291–11295 (2019).
7. Gallagher NM, Olankitwanit A, Rajca A. High-spin organic molecules. *J. Org. Chem.* **80**, 1291–1298 (2015).
8. Sun Z, Zeng Z, Wu J. Zethrenes, Extended p-Quinodimethanes, and Periacenes with a Singlet Biradical Ground State. *Acc. Chem. Res.* **47**, 2582–2591 (2014).
9. Liu C, Ni Y, Lu X, Li G, Wu J. Global aromaticity in macrocyclic polyradicaloids: hackers rule or baird's rule? *Acc. Chem. Res.* **52**, 2309–2321 (2019).
10. Rudebusch GE, Zafra JL, Jorner K, Fukuda K, Marshall JL, Arrechea-Marcos I, *et al.* Diindeno-fusion of an anthracene as a design strategy for stable organic biradicals. *Nat. Chem.* **8**, 753–759 (2016).
11. Li Y, Li L, Wu Y, Li Y. A Review on the Origin of Synthetic Metal Radical: Singlet Open-Shell Radical Ground State? *J. Phys. Chem. C* **121**, 8579–8588 (2017).
12. Dediu VA, Hueso LE, Bergenti I, Taliani C. Spin routes in organic semiconductors. *Nat. Mater.* **8**, 707–716 (2009).
13. Tsurumi J, Matsui H, Kubo T, Hausermann R, Mitsui C, Okamoto T, *et al.* Coexistence of ultra-long spin relaxation time and coherent charge transport in organic single-crystal semiconductors. *Nat. Phys.* **13**, 994–998 (2017).
14. Fratini S, Nikolka M, Salleo A, Schweicher G, Sirringhaus H. Charge transport in high-mobility conjugated polymers and molecular semiconductors. *Nat. Mater.* **19**, 491–502 (2020).
15. Kubo T, Shimizu A, Sakamoto M, Uruichi M, Yakushi K, Nakano M, *et al.* Synthesis, intermolecular interaction, and semiconductive behavior of a delocalized singlet biradical hydrocarbon. *Angew. Chem., Int. Ed.* **44**, 6564–6568 (2005).
16. Zhang Y, Zheng Y, Zhou H, Miao M-S, Wudl F, Thuc-Quyen N. Temperature tunable self-doping in stable diradicaloid thin-film devices. *Adv. Mater.* **27**, 7412–7419 (2015).
17. Wang W, Ge L, Xue G, Miao F, Chen P, Chen H, *et al.* Fine-tuning the diradical character of molecular systems via the heteroatom effect. *Chem. Commun.* **56**, 1405–1408 (2020).
18. Guo X, Facchetti A. The journey of conducting polymers from discovery to application. *Nat. Mater.* **19**, 922–928 (2020).
19. Venkateshvaran D, Nikolka M, Sadhanala A, Lemaur V, Zelazny M, Kepa M, *et al.* Approaching disorder-free transport in high-mobility conjugated polymers. *Nature* **515**, 384–388 (2014).
20. Wang S, Xu J, Wang W, Wang G-JN, Rastak R, Molina-Lopez F, *et al.* Skin electronics from scalable fabrication of an intrinsically stretchable transistor array. *Nature* **555**, 83–88 (2018).

21. Guo X, Facchetti A, Marks TJ. Imide- and amide-functionalized polymer semiconductors. *Chem. Rev.* **114**, 8943–9021 (2014).
22. Yang J, Zhao Z, Wang S, Guo Y, Liu Y. Insight into high-performance conjugated polymers for organic field-effect transistors. *Chem* **4**, 2748–2785 (2018).
23. Lei T, Wang J-Y, Pei J. Design, synthesis, and structure-property relationships of isoindigo-based conjugated polymers. *Acc. Chem. Res.* **47**, 1117–1126 (2014).
24. Lei T, Xia X, Wang J-Y, Liu C-J, Pei J. "Conformation locked" strong electron-deficient poly(p-phenylene vinylene) derivatives for ambient-stable n-type field-effect transistors: synthesis, properties, and effects of fluorine substitution position. *J. Am. Chem. Soc.* **136**, 2135–2141 (2014).
25. Schott S, Chopra U, Lemaur V, Melnyk A, Olivier Y, Di Pietro R, *et al.* Polaron spin dynamics in high-mobility polymeric semiconductors. *Nat. Phys.* **15**, 814–822 (2019).
26. Boyle CJ, Upadhyaya M, Wang P, Renna LA, Lu-Díaz M, Pyo Jeong S, *et al.* Tuning charge transport dynamics via clustering of doping in organic semiconductor thin films. *Nat. Commun.* **10**, 2827 (2019).
27. London AE, Chen H, Sabuj MA, Tropp J, Saghayezhian M, Eedugurala N, *et al.* A high-spin ground-state donor-acceptor conjugated polymer. *Sci. Adv.* **5**, eaav2336 (2019).
28. Vella JH, Huang L, Eedugurala N, Mayer KS, Ng TN, Azoulay JD. Broadband infrared photodetection using a narrow bandgap conjugated polymer. *Sci. Adv.* **7**, DOI: 10.1126/sciadv.abg2418 (2021).
29. Sun H, Guo X, Facchetti A. High-performance n-type polymer semiconductors: applications, recent development, and challenges. *Chem* **6**, 1310–1326 (2020).
30. Che Y, Perepichka DF. Quantifying Planarity in the Design of Organic Electronic Materials. *Angew. Chem., Int. Ed.* **60**, 1364–1373 (2021).
31. Ji X, Xie H, Zhu C, Zou Y, Mu AU, Al-Hashimi M, *et al.* Pauli paramagnetism of stable analogues of pernigraniline salt featuring ladder-type constitution. *J. Am. Chem. Soc.* **142**, 641–648 (2020).
32. Kang K, Watanabe S, Broch K, Sepe A, Brown A, Nasrallah I, *et al.* 2D coherent charge transport in highly ordered conducting polymers doped by solid state diffusion. *Nat. Mater.* **15**, 896–902 (2016).
33. Tanaka H, Hirate M, Watanabe S, Kuroda S-i. Microscopic signature of metallic state in semicrystalline conjugated polymers doped with fluoroalkylsilane molecules. *Adv. Mater.* **26**, 2376–2383 (2014).
34. Kang K, Watanabe S, Broch K, Sepe A, Brown A, Nasrallah I, *et al.* 2D coherent charge transport in highly ordered conducting polymers doped by solid state diffusion. *Nat. Mater.* **15**, 896–902 (2016).
35. Xiong M, Yan X, Li J-T, Zhang S, Cao Z, Prine N, *et al.* Efficient n-Doping of Polymeric Semiconductors through Controlling the Dynamics of Solution-State Polymer Aggregates. *Angew. Chem., Int. Ed.* **60**, 8189–8197 (2021).
36. Hu H, Chow PCY, Zhang G, Ma T, Liu J, Yang G, *et al.* Design of Donor Polymers with Strong Temperature-Dependent Aggregation Property for Efficient Organic Photovoltaics. *Acc. Chem. Res.* **50**, 2519–2528 (2017).

37. Steyrleuthner R, Schubert M, Howard I, Klaumuenzer B, Schilling K, Chen Z, *et al.* Aggregation in a high-mobility n-type low-bandgap copolymer with implications on semicrystalline morphology. *J. Am. Chem. Soc.* **134**, 18303–18317 (2012).
38. Yamaguchi K, Fueno T, Fukutome H. Molecular-orbital theoretical classification of reactions of singlet ground-state molecules. *Chem. Phys. Lett.* **22**, 461–465 (1973).
39. Zeng W, Phan H, Herng TS, Gopalakrishna TY, Aratani N, Zeng Z, *et al.* Rylene Ribbons with Unusual Diradical Character. *Chem* **2**, 81–92 (2017).
40. Koike H, Chikamatsu M, Azumi R, Tsutsumi Jy, Ogawa K, Yamane W, *et al.* Stable delocalized singlet biradical hydrocarbon for organic field-effect transistors. *Adv. Funct. Mater.* **26**, 277–283 (2016).
41. Noriega R, Rivnay J, Vandewal K, Koch FPV, Stingelin N, Smith P, *et al.* A general relationship between disorder, aggregation and charge transport in conjugated polymers. *Nat. Mater.* **12**, 1038–1044 (2013).
42. Lei T, Dou J-H, Pei J. Influence of Alkyl Chain Branching Positions on the Hole Mobilities of Polymer Thin-Film Transistors. *Adv. Mater.* **24**, 6457–6461 (2012).
43. Fornari RP, Blom PWM, Troisi A. How Many Parameters Actually Affect the Mobility of Conjugated Polymers? *Phys. Rev. Lett.* **118**, 086601 (2017).
44. Wang Y, Rogado NS, Cava RJ, Ong NP. Spin entropy as the likely source of enhanced thermopower in NaxCo2O4. *Nature* **423**, 425–428 (2003).
45. Tam TLD, Wu G, Chien SW, Lim SFV, Yang S-W, Xu J. High Spin Pro-Quinoid Benzo 1,2-c;4,5-c ' bisthiadiazole Conjugated Polymers for High-Performance Solution-Processable Polymer Thermoelectrics. *ACS Mater. Lett.* **2**, 147–152 (2020).
46. Yan X, Xiong M, Li J-T, Zhang S, Ahmad Z, Lu Y, *et al.* Pyrazine-Flanked Diketopyrrolopyrrole (DPP): A New Polymer Building Block for High-Performance n-Type Organic Thermoelectrics. *J. Am. Chem. Soc.* **141**, 20215–20221 (2019).
47. Lu Y, Yu Z-D, Liu Y, Ding Y-F, Yang C-Y, Yao Z-F, *et al.* The Critical Role of Dopant Cations in Electrical Conductivity and Thermoelectric Performance of n-Doped Polymers. *J. Am. Chem. Soc.* **142**, 15340–15348 (2020).
48. Russ B, Glaudell A, Urban JJ, Chabinyc ML, Segalman RA. Organic thermoelectric materials for energy harvesting and temperature control. *Nat. Rev. Mater.* **1**, 17086 (2016).
49. Zhang F, Di C-a. Exploring Thermoelectric Materials from High Mobility Organic Semiconductors. *Chem. Mater.* **32**, 2688–2702 (2020).
50. Rivnay J, Inal S, Salleo A, Owens RM, Berggren M, Malliaras GG. Organic electrochemical transistors. *Nat. Rev. Mater.* **3**, 16050 (2018).
51. Zeglio E, Inganas O. Active Materials for Organic Electrochemical Transistors. *Adv. Mater.* **30**, 1800941 (2018).

Figures

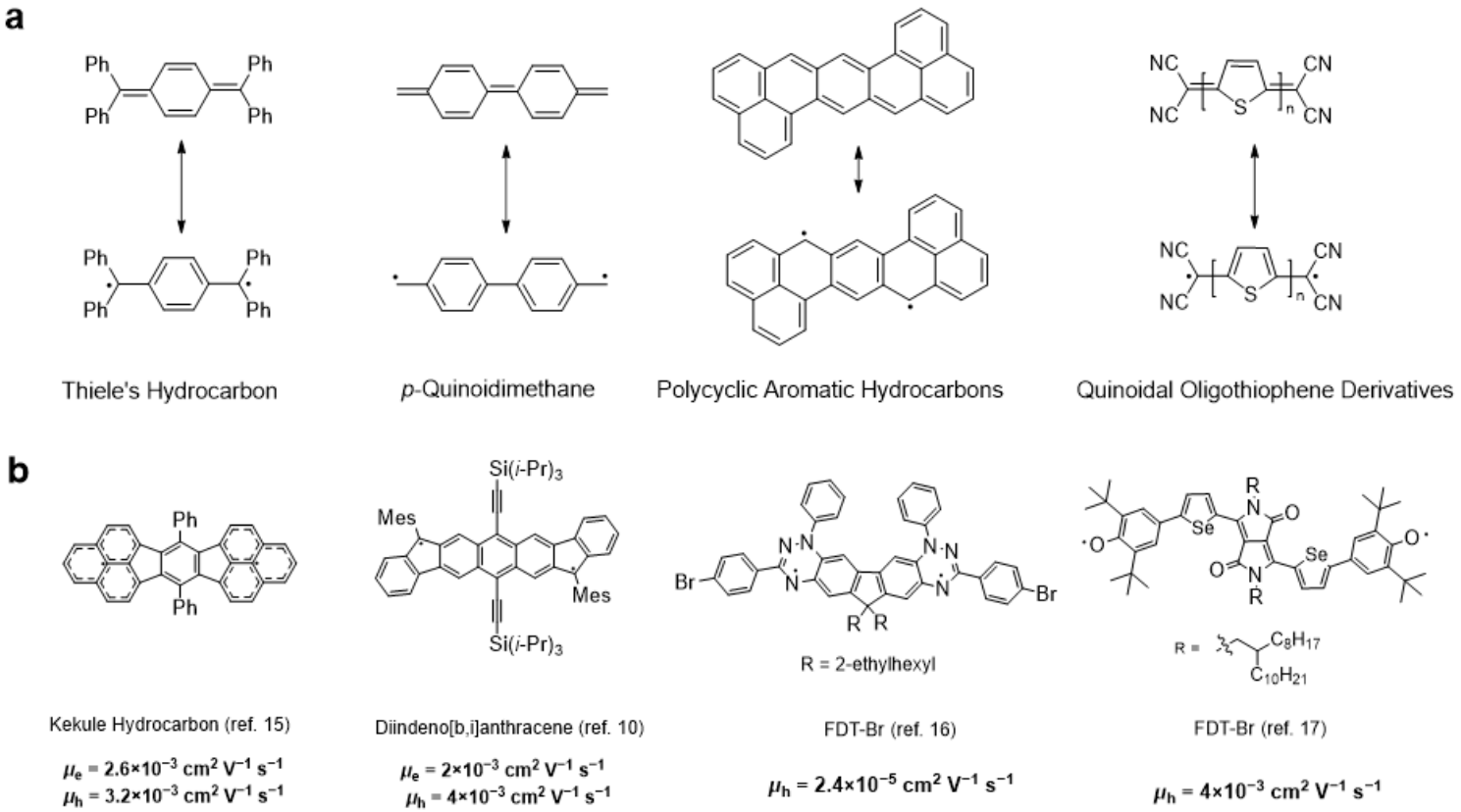

Figure 1

Previous works on the design and synthesis of open-shell or high-spin π-conjugated organic molecules. a, Resonance structures of several open-shell π-conjugated molecule building blocks. b, Some representative open-shell or high-spin organic semiconductors and their charge carrier mobilities.

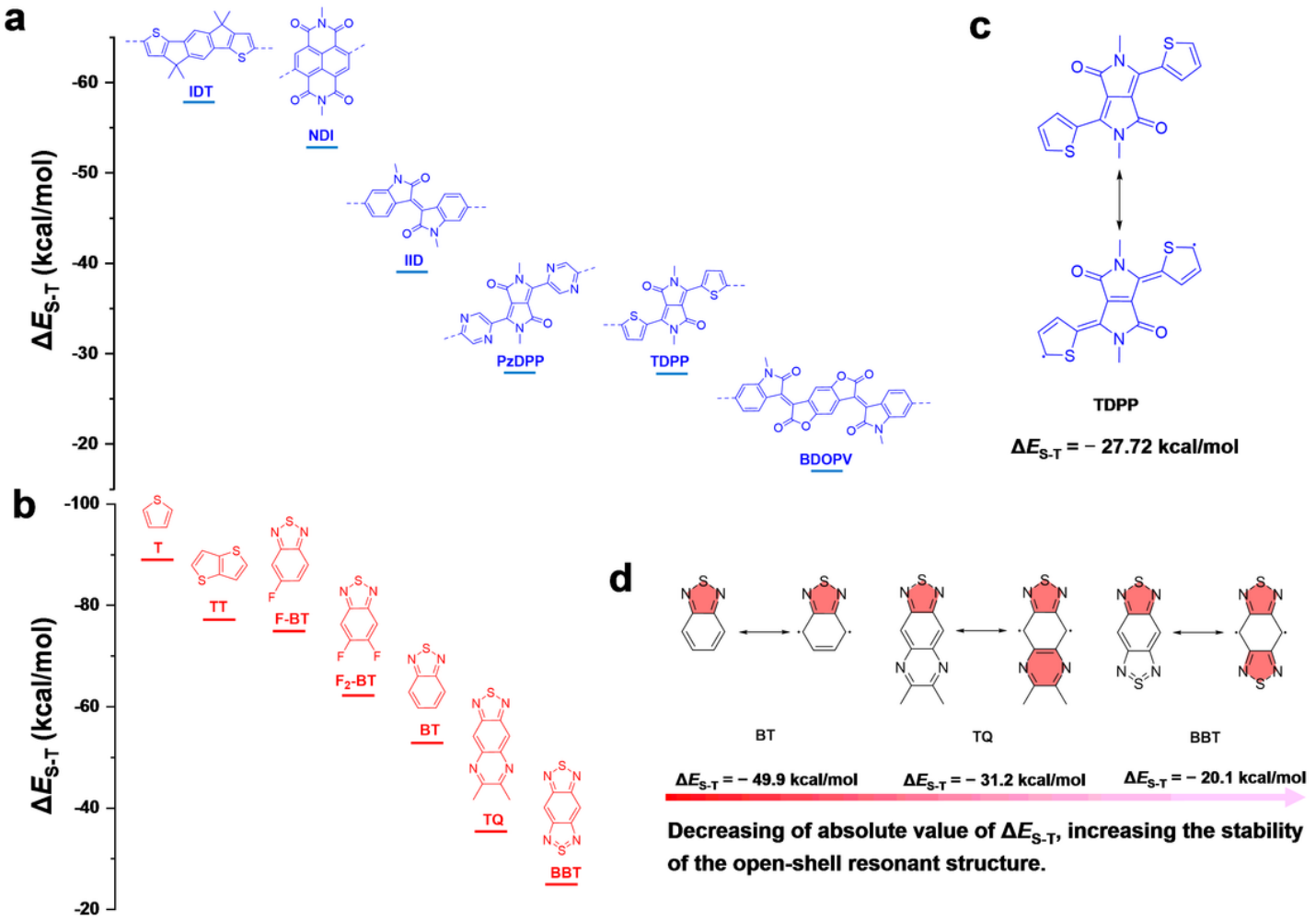

Figure 2

Computer-aided polymer building block screening approach to rational design of high-spin ground-state semiconducting polymers. DFT Calculated ΔES-T values of a, “large fused aromatic” and b, “small-size aromatic” building blocks used in high-mobility semiconducting polymers; c, The closed-shell and open-shell resonance structures of TDPP. d, The closed-shell and open-shell resonance structures of BT, TQ, and BBT.

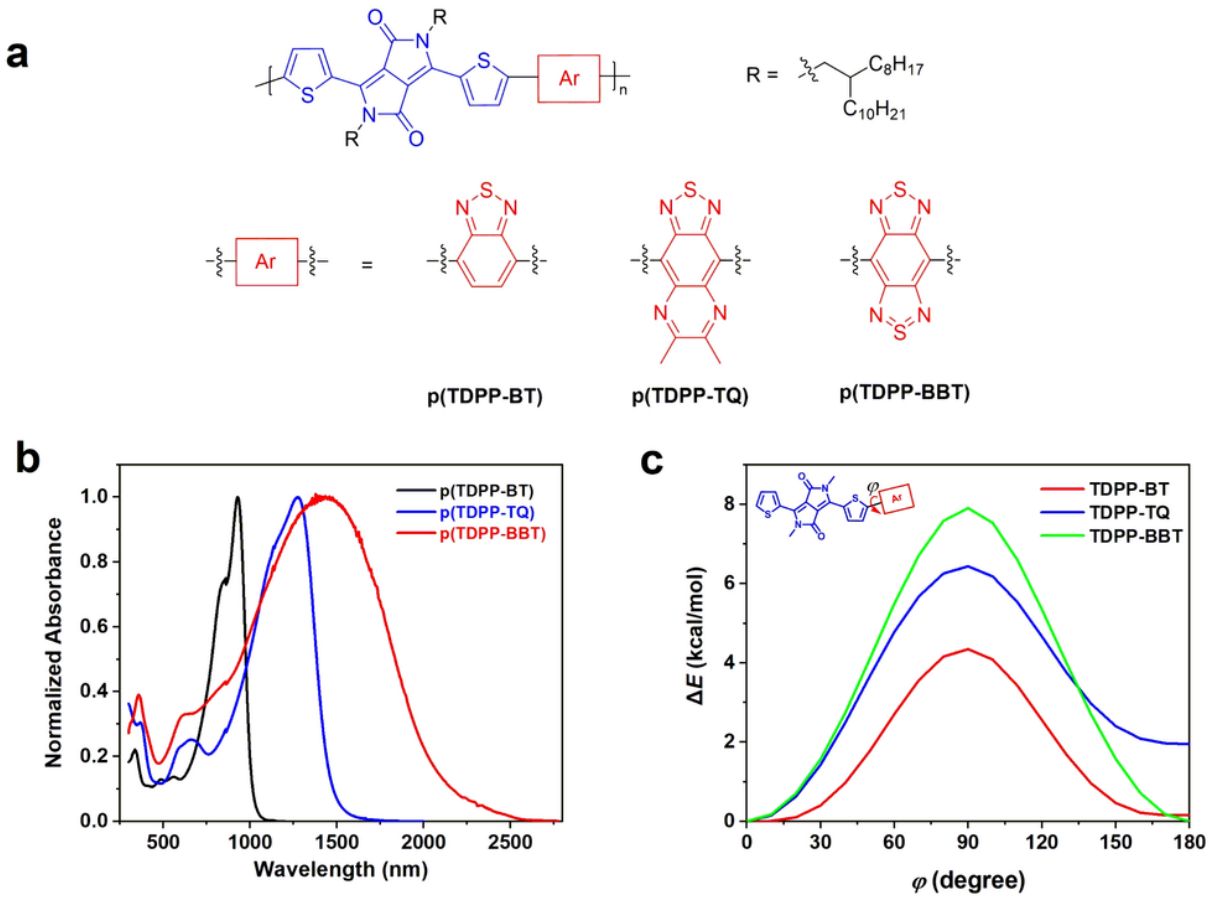

Figure 3

Chemical structure and characterization. a, Molecular structures of the high-spin ground-state semiconducting polymers. b, UV-vis-NIR absorption spectra of the polymers in ODCB solution (1 × 10−5 M). c, Calculated potential energy scans (PES) of the dihedral angles φ between the TDPP and three BT derivatives.

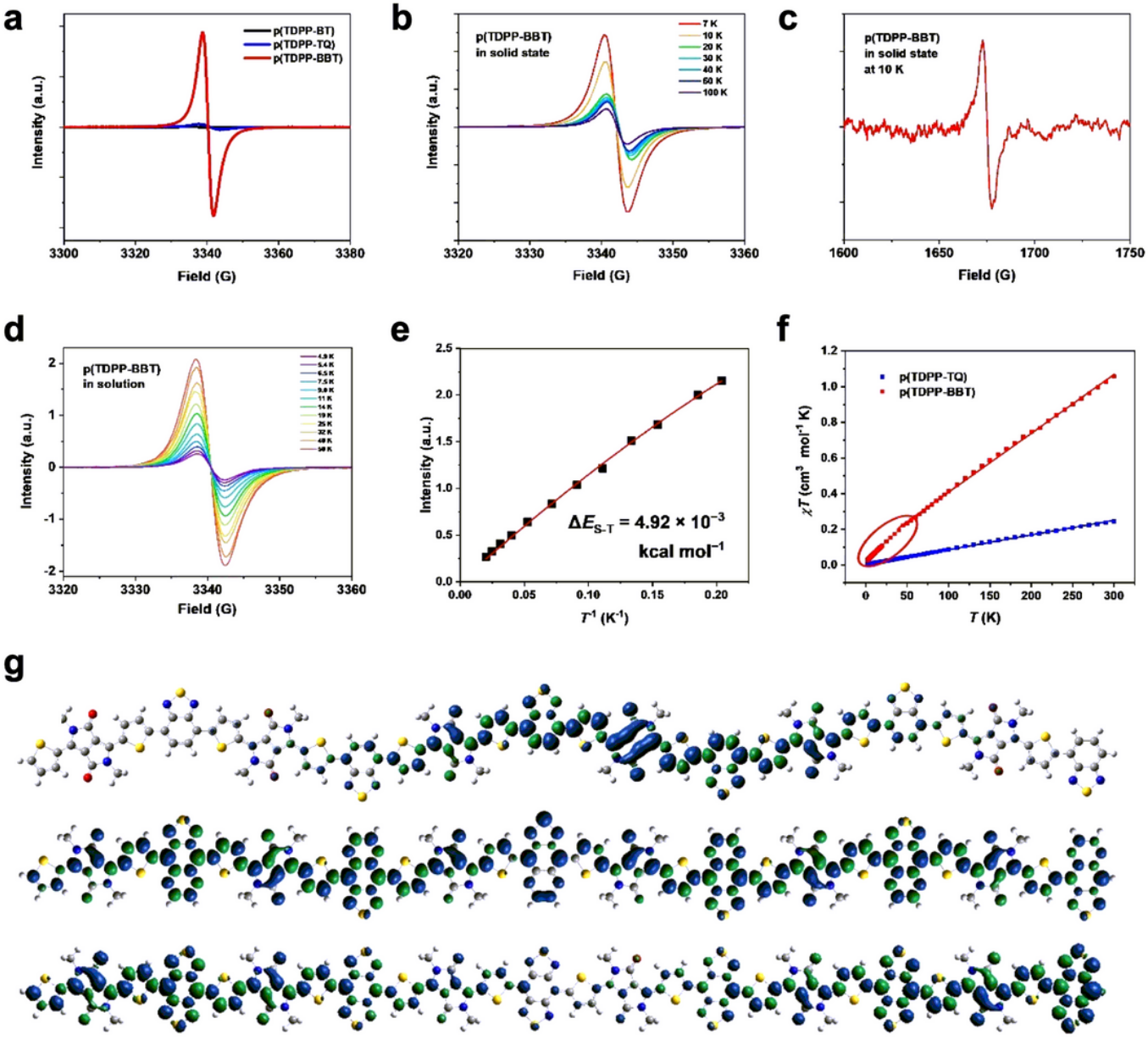

Figure 4

Magnetic property characterization and DFT calculation. a, Room temperature EPR signals of the polymers in solid state; b, Variable temperature EPR of p(TDPP-BBT) in solid state; c, the half field line of p(TDPP-BBT) in solid state; d, Temperature-dependent EPR of p(TDPP-BBT) in 1×10−3 M o-xylene and e, the corresponding Bleaney-Bowers equation fitting result; f, Temperature-dependent magnetic susceptibility from 2 K to 300 K. Solid squares are data, solid lines are linear fitting lines. g, Spin density distribution of the triplet states of the oligomers (n = 6) of p(TDPP-BT) (top), p(TDPP-TQ) (middle), p(TDPP-BBT) (bottom). DFT calculation were performed at the UB3LYP/6-31G** level.

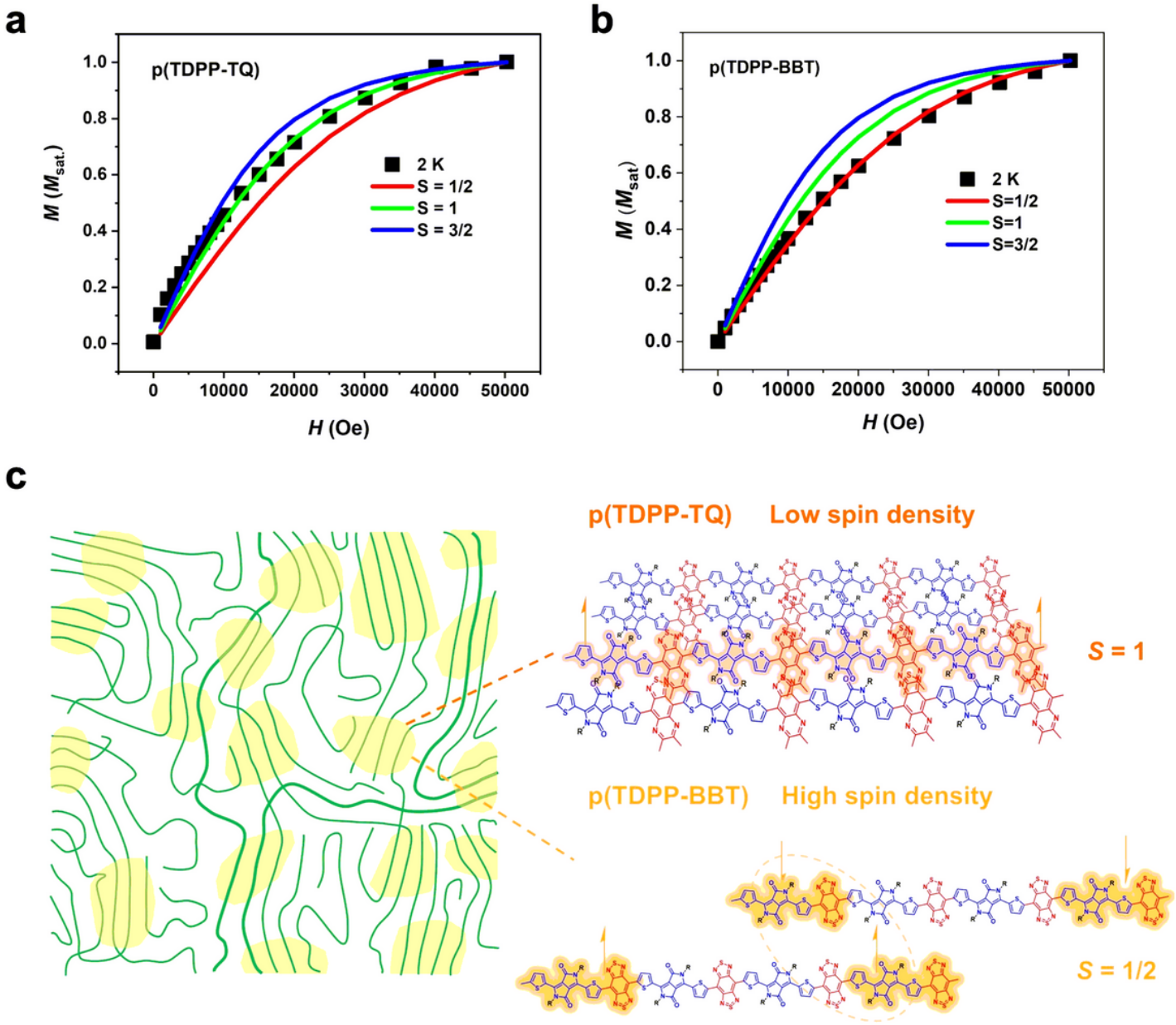

Figure 5

Magnetic characterization and the mechanism explanation of the different spin ground states of high-spin polymers. Measuement Field dependent magnetization of a, p(TDPP-TQ) and b, p(TDPP-BBT) from 0 Oe to 50000 Oe. The solid squares are the experimental data, the solid lines stand for the simulated curve by Brillouin equation. The simulation results exhibit the S = 1 and S = 1/2 ground states of p(TDPP-TQ) and p(TDPP-BBT). c, Schematic illustration of the mechanism of the different ground states of p(TDPP-TQ) and p(TDPP-BBT). Both polymers have strong interchain interactions in solid state. p(TDPP-TQ) has low spin density and exhibited triplet ground state. p(TDPP-BBT) has high spin density and exhibited doublet ground state due to the strong spin-spin interactions.

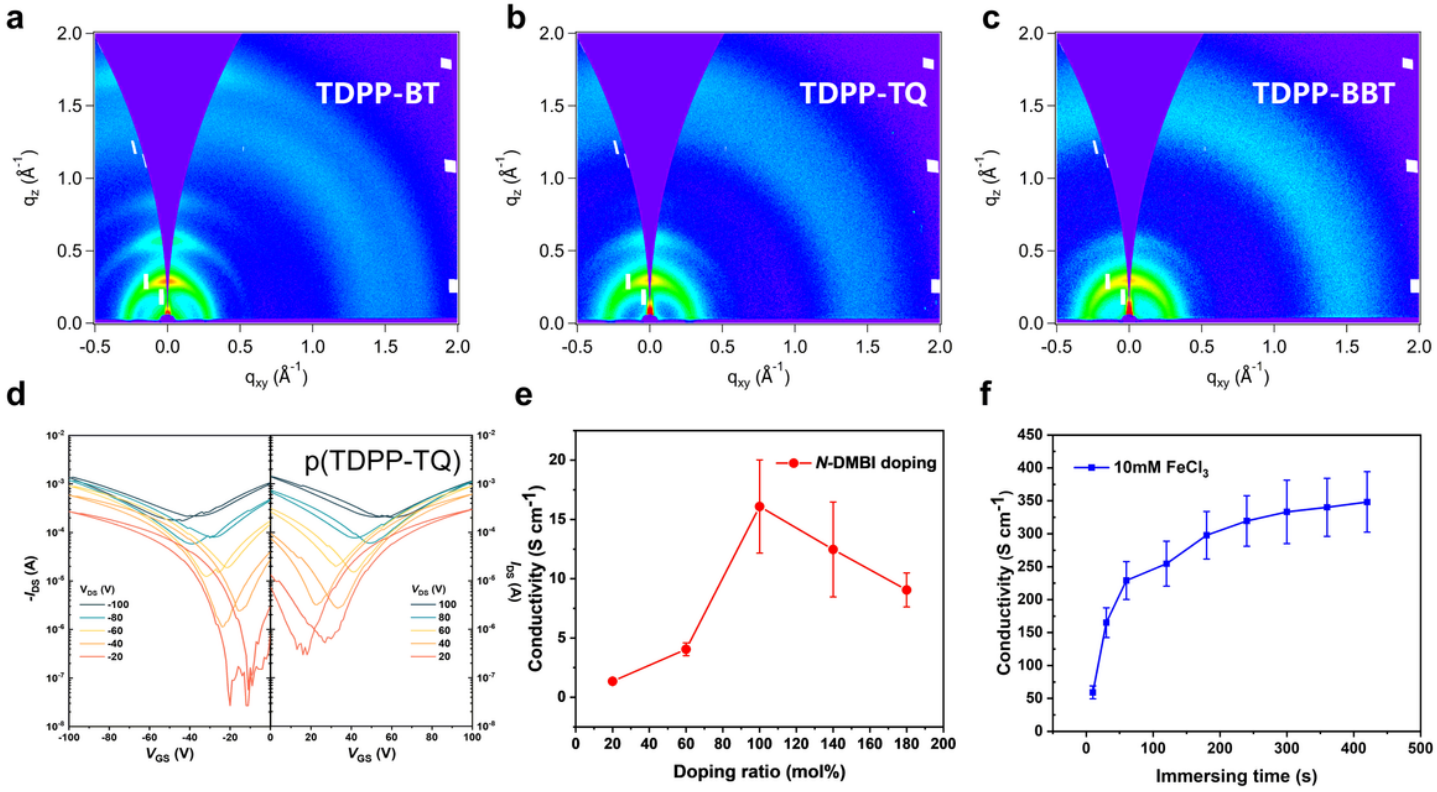

Figure 6

Thin film morphology and device characterization. 2D-grazing incidence wide-angle X-ray scattering (GIWAXS) pattern of a, p(TDPP-BT), b, p(TDPP-TQ), c, p(TDPP-BBT). d, Typical transfer characteristics of a p(TDPP-TQ) FET device. e, N-type electrical conductivities of p(TDPP-TQ) doped by N-DMBI with different ratios.; f, P-type electrical conductivities of p(TDPP-TQ) doped by immersing in 10 mM FeCl3 solution.

Supplementary Files

This is a list of supplementary files associated with this preprint. Click to download.

- ManuscriptforHighspinpolymers20210730SI.docx